INTERNATIONAL JOURNAL OF INNOVATIVE RESEARCH & DEVELOPMENT

ISSN 2278 – 0211 (Online)

Modelling and Analysis of Urban Growth of Idah Metropolis Using GIS Integrated Gradient Technique

Fatima Adamu
Chief Technologist, Department of Surveying and Geoinformatics
Federal Polytechnic Idah, Kogi State, Nigeria
Joel Izuchukwu Igbokwe
Professor, Department of Surveying and Geoinformatics,
Nnamdi Azikiwe University, Awka, Nigeria

Abstract:
This thesis aims to better understand changes in the spatial pattern of urban growth and its impact on landscape configuration by conducting a case study in Idah metropolis. The objectives are as follows:

- *To model and analyze multi-temporal images (2001, 2010, and 2021) for determining the urban growth in Idah,*
- *To determine urban development trends using post-classification comparisons,*
- *Evaluating the degree of urban growth according to urban land cover change over that period*

Satellite imagery was employed to distinguish and identify different land surface categories. Integrated remote sensing and GIS (Geographic Information System) technique was used to analyse both qualitative and quantitative perspectives regarding the objectives. The results indicate that the urban area of Idah experienced changes in the various classes. The vegetated area experienced a great change of 49.98%. That is a decrease from the previous year of 2001 to 2010. Also, another 48.67% decrease from 2010 to 2021 is due to the developments in the study area. The built-up area equally decreased by 1.33 % between 2010 and 2021. There was an increase of 12.04% from the year 2001 to 2010.Beach has a drastic increase from 28.10% observed between 2001 and 2010 to 44.50% between 2010. The geographic footprint demonstrates that the distribution of the built-up area was dispersed and continues to grow more dispersed. The significant contribution of this study could benefit many aspects, such as comparative studies between cities or continuous studies relevant to urban growth.

Keywords: *Urban growth, remote sensing, GIS*

1. Introduction

1.1. Background Information for the Study

The urban environment has been rapidly changing in the last few decades due to population growth and emigration from rural to urban areas. The urban environment has changed drastically over the past few decades. The rate at which a city's population grows is called urban growth. Urbanization, or the transfer of people from rural to urban regions, is the cause of this. Urbanization may result in increased economic development (Elizabeth et al., 2014). A metropolitan or suburban area's expansion is sometimes referred to as urban growth. Urbanization has grown dramatically as a global phenomenon over the past century. In recent decades, urban expansion has increased due to population movement, particularly in emerging nations (UNEP, 2005). By 2030, it is predicted that more than 60% of the world's population will live in cities, based on the rate of current growth (Moeller & Blasclake, 2006; Odind & Mhangara, 2012).This expansion has a natural tendency to spread out in various ways. However, sudden, unplanned urban growth could pose a serious problem if the necessary foundation is not laid properly. In order to administer the urban region, decision-makers and planners should implement a decision support system. Degradation, urban development, and priceless consumption and production tendencies are the results. According to Yenolde & Cobral (2011), greater than the actual urban population growth is found in the metropolitan area. Cities are putting a lot of strain on available resources and land due to their fast growth. Reflect et al. (2009); Leoa et al. (2004). Inadequate housing, environmental degradation, crime, traffic congestion, and other concerns will result if this is not addressed (Subasinghe et al., 2016)

Boori (2016) suggested using an all-encompassing strategy to consistently investigate and analyze urban growth. Geographical information systems and remote sensing can provide data on urban expansion and its modeling to help understand urban problems. Within a single system, GIS offers several spatial information components. Giving data a visual representation is the main purpose of a geographic information system. Urban growth and its trajectory are analyzed and modelled using GIS technology. Current and accurate land use information is essential for managing spatial planning in the comprehensive land use planning of metropolitan regions. It is vital to monitor urban growth in Idah to adopt suitable methods for the urban planning decision-making process and revise urban policies.

2. Study Area

With an estimated population of 79,815 (NPC, 2006) and a 36 km^2 area, Idah is a local government area in Kogi State, Nigeria. It is situated between Latitude 07^0 02' 30"N and 07 ^{0} 09 '30"N of the equator and between Longitude 06 ^{0}42 '00"E and 06 ^{0}46' 30"E of the Greenwich meridian.

3. Method

Requirement and sources for data: The information needed to accomplish the study's goal and objectives will be divided into primary and secondary sources.

The main information: GPS-based field data with ground truth coordinates.

The secondary information: Earth Explorer will be used to download low-resolution satellite images of the study region from the USGS for the years 2001, 2010, and 2021 (land sat 5 TM, land sat 7 ETM +, and land sat 8 ETM+).

From the Kogi State ministry of land, survey, and urban development, the study area map will be received in analog format and scanned into the computer using an Adobe Photoshop scanner.

3.1. Requirements for Hardware and Software

This refers to the hardware and software used to collect, store, process, analyze, and display the contents of spatial data.

3.1.1. Requirements for Hardware

- A Laptop with 100GB of hard drive capacity, 8GB of RAM, and a 1.75GHz processor.
- A GPS to locate features during a field verification exercise (Garmn76 handheld GPS)
- A4-size reports, colored photos, and maps can be printed using an HP Deskjet printer.
- An HP AO scanner can be used to digitize hardcopy maps.

3.1.2. Required Software and Other Equipment

The following software has been taken into consideration and found to be useful in attaining the project's objective.

ArcGIS 10.5, which is going to be utilized for GIS analysis. To perform picture categorization, change detection, and accuracy evaluation, ERDAS IMAGINE 9.2 will be used.

Microsoft Word will be employed in the creation of the reports.

Microsoft Excel will be used to generalize the regression and display statistical data on land cover.

3.2. Modelling and Processing for Data Acquisition

According to The United States Geological Survey (USGS), Earth Explorer will be used to provide an internet image portal from which the metrology used in this investigation will be obtained. Strategies will be implemented for classifying remote sensing images, spatiotemporal analysis of satellite images, and logistic regression. Using the maximum likelihood classification technique in ERDAS pictures, the land cover map will be created from the first three (3) multi-temporal sets of photos spanning the study area. To create a growth change map, 9.2 post-classification comparisons are suggested. This would involve using several spatial analyst tools in ArcGIS 10.8 to layer the classification images on top of one another. The Kogi state political map will be utilized.

3.3. Image Acquisition

The study's primary data, including the Landsat 7 ETM picture from 2001 and the LandSat 8 OLI image from 2010 to 2021, were downloaded from the USGS website using Earth Explorer. Additionally, real-world data were used to assess accuracy.

3.4. Satellite Image Data

The table below displays the characteristics of the satellite images used:

S/N	Year	Satellite	Sensor	Resolution	Path/Row	Date Captured
1	2001	Landsat 7	ETM	30m	189/055	30/12/2001
2	2010	Landsat 8	OLI	30m	189/055	23/12/2010
3	2021	Landsat 8	OLI	30m	189/055	06/01/2021

Table 1: Displays the Attributes of the Satellite Pictures

3.5. Image Pre-processing

This refers to the processes that the images were subjected to be ready for image classification.

3.5.1. Enhancement of Images and Band Combinations

To enhance the quality of the image as seen by a human, image enhancement techniques were used. By adding more visual interpretation to the data, the technique seeks to alter the original image data and produce a 'new' image. For this project, a band combination was utilized. This method is especially useful because many satellite photos do not provide enough information for image interpretation when viewed on a color display. The proper RGB bands of each image were blended to obtain the true/natural color of each Landsat image. For the Landsat 8 image, use bands 7, 5, and 3, and for the Landsat 7,use ETM.

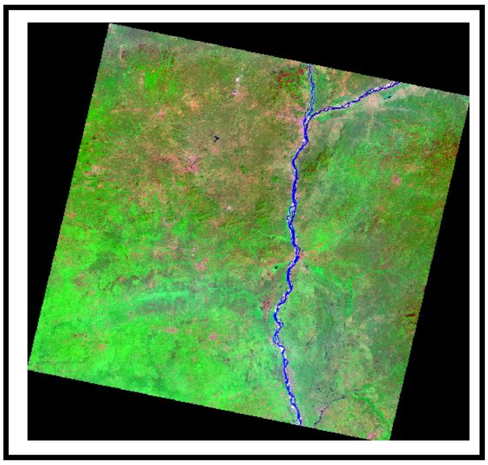

Figure 1: Composite Image for Landsat 7(2001)

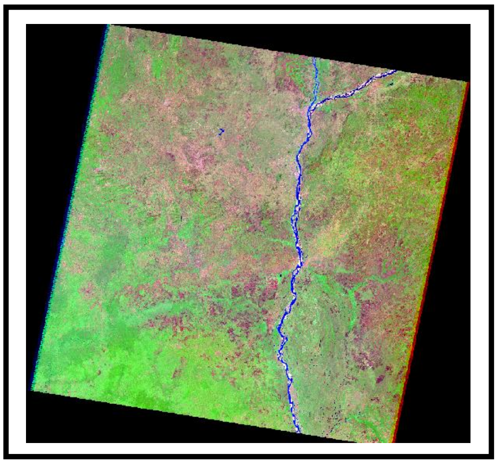

Figure 2: Composite Image for Landsat 8(2010)

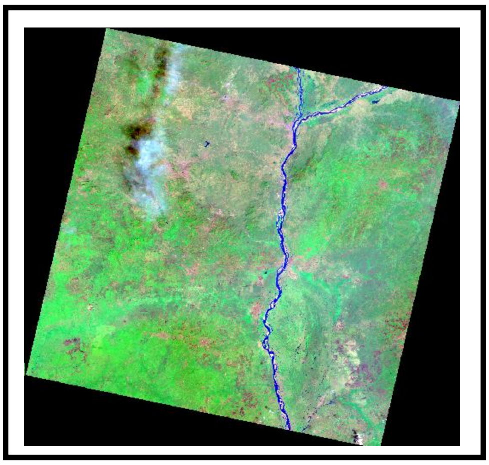

Figure 3: Composite Image for Landsat 8(2021)

3.5.2. Image Subsetting

One Landsat picture spans roughly 170 km in the north and south and 183 km in the east and west (106 mi by 114 mi). Due to its size, the study region was reduced or excised from the scene using ArcMap's "Clip" tool and its shapefile as a reference.

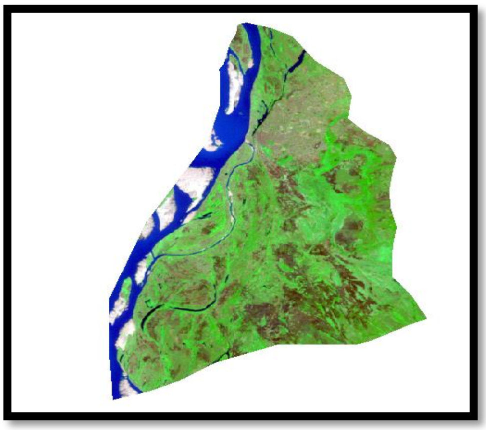

Figure 4: Subset of Landsat 7 (2001)

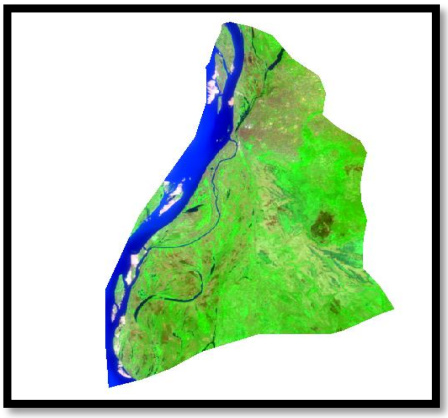

Figure 5: Subset of Landsat 8 (2010)

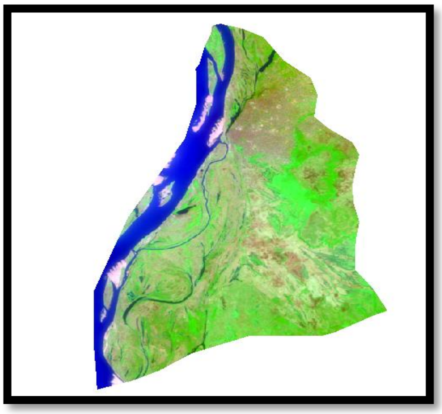

Figure 6: Subset of Landsat 8 (2021)

3.5.3. Stage of Training

The process of gathering similar pixels for the program to utilize in identifying the photos is known as the training stage. It was extensively inspected to ascertain that the image would be classified into many classes. Built-up areas, water bodies, vegetation, and bare terrain were the land cover/land use classes recognized. The procedure used by ERDAS entails: The Signature Editor window is necessary to gather training samples under the Raster tab.

3.5.4.Supervised | Signature Editor

- Under the AOI menu at the top of the interface, click the Drawing tab. This opens the AOI tools, which can be used to collect the samples,
- In the Insert Geometry section, select the Polygon tool,
- Zoom in on the image, digitize around the pixels, and add it to the Signature Editor window by clicking the Create New Signature from the AOI icon,
- When more than one sample is collected from the class, highlight/select all the samples, and click on the Merge Selected Signatures icon on the Signature Editor Window to merge the samples into one. Assign a class name. After collection, the training samples are saved as a signature file that the program uses to classify the image.

3.6. Image Classification

There are two different forms of classification based on how the computer and interpreter interact throughout the classification process. Supervised and Unsupervised Classification Methods are the two basic categories utilized to provide classed output.In supervised classification, the user or image analyst 'supervises' the pixel classification process. The supervised classification is generally chosen when an analyst has good knowledge of the area; in supervised classification, the analyst selects representative samples for each land cover class. The software then uses these 'training sites' and applies them to the entire image. Supervised classification uses the spectral signature defined in the training set. The multispectral data from the pixels in the sample area or spectral signatures from the spectral library will train a classification algorithm (Kamaruzaman*et al.,* 2009). Once trained, the algorithm will then be applied to the entire image, and a final classification image will be obtained.

The algorithm used in this project is the Maximum Likelihood. The classifications were done using Erdas Imagine 2001.

ERDAS IMAGINE 9.2 was engaged in doing the image pre-processing, classification, and accuracy assessment. In performing image classification, a maximum likelihood classifier was employed in the supervised classification, and adopting and modifying Anderson Level-I Scheme was used to control the classes (Anderson et al., 1976). For this work, four categories were employed: Beach, Build-up area, Vegetation, and Waterbodies, as presented in table 2, showing the different land use and land cover categories.

A classified map was used for sample training and for assessing classification accuracy for the 2001 classified map, while the ground truth information acquired in the field was used for the same process for the 2010 classified map.

After this operation, a post-classification technique was used to minimize classification errors due to the connections in the spectral signature. Accuracy assessment was accompanied by using a stratified random sample process. Three hundred randomly selected points were generated, of which 100 were used to do the supervised classification, and the rest were used for accuracy assessment.

The reference data for the 2021 OLI image was gathered from two sources: Fieldwork and Expert knowledge.

GPS point fieldwork served as reference information for the purpose of validation. In the fieldwork, 200 samples were collected: 100 samples were used for the classification training and the rest for the accuracy assessment.

Categories	**Definition**
Waterbodies	River, Streams, reservoir
Vegetation	Palm plantations, dry cropland, grass
Built-up areas	Built-up Areas,i.e., Residential, commercial services, industrial, transportation, mixed urban or built-up land, other urban or built-up lands
Beach	Floodplain, construction area

Table 2: The Definition of Land Use Classes
Source: Own Illustration; Based on Anderson Et Al., 1976

3.7. Maximum Likelihood Classification (MLC)

The Maximum Likelihood Classification tool's approach is based on Bayes' selection theorem, which states that the cells within every class sample in multidimensional space are evenly distributed. While allocating each cell to one of the classes described in the signature file, the Maximum likelihood classification approach uses both the variances and co-variances of the class signatures.

MLC was used to extract land cover information and create a distance image from Landsat data. MLC created a classified image with four categories to examine the impact of seasonal changes on urban, built-up land, vegetation, and water body—the Mahalanobis distance between the equivalent pixel in the input continuous raster layer file and the classified signature. The pixels which are most susceptible to being misidentified have a greater value in the distance image data. A few pixels were misinterpreted in the preliminary classification results following MLC-supervised classification because of the Landsat images, somewhat fine spatial resolution, and spectral similarity. The statistical likelihood for each category is estimated using these two features for each cell value to identify the cells' placement in the class. When an a priori selection is chosen, The Bayesian solution is used to compute the weighted distance or likelihood D of an unexpected measurement vector X belonging to one of the predefined sequences.

MLC is a Bayes theorem-based supervised image classification algorithm. In a previous paper, the algorithm and implementation of MLC on several platforms were addressed in detail (Shi & Xue, 2017). In a nutshell, MLC calculates the likelihood that a pixel with feature vector x belongs to a class and allocates it to the most appropriate class. The equation is as follows: (Richards & Jia, 1999)

$$p(\omega_i / x) = p(x / \omega_i) * p(\omega_i) / p(x)$$

Where x denotes a pixel, if the image has many bands, at that moment, x would be a vector. P (ωi) is the likelihood that class ωiarises in the image. It is calculated from the training data, allocated indiscriminately, or considered to be equal throughout all categories. It is indeed essential to determine a probability threshold beneath which no categories are allocated to the pixel. P($x/\omega i$), the probability of detecting x in class ωi can result from the training data.

Hence,

$X \in \omega_i \text{if}$

$p(x/\omega_i)*p(\omega_i) > p(x/\omega_j)*p(\omega_j)$

for all j=~~i~~

MLC considers that the distribution of digital pixel values follows a multivariate normal distribution, which is **p (x/ωi) N(ui),** which leads to maximum likelihood approximation of **p (wi/x)**

$$p(\omega_i / x) = 2\pi^{-N/2}[C_i]^{-1/2} e^{-\frac{1}{2}}(x - mi)^t C_i^{-1}(x - m_i)$$

Captivating log on both sides, the above equation is interpreted as,

$$g_i(x) = \ln p(\omega_i) - \frac{1}{2}\ln C_i (x - m_i)^t C^{-1}{}_i (x - m_i)$$

Since it decides the class label of pixel **x**, **Equation 1** is known as the determinant value. In class **I, Ci** and **mi** are sample measures of co-variance and mean. The probability that **x** falls to class **I**is given by **gix.** Even though MLC is a linear computational technique, the processing time for a big remote-sensing image may be inaccessible.

4. Presentation and Discussion of Results

In this chapter, the results of the Land cover /Land use classifications, Post classification, change detection, and accuracy assessments were presented and compared.

Table 3 shows the confusion matrix for the classification. It indicates that the overall classification accuracy of land use maps is 96.10% for 2001 and 99.68% for 2010. The Kappa coefficients for the maps of 2001 and 2010 are 0.91 and 0.99, respectively. The producer's accuracy ranged from 93.22% to 100% (93.22%; 83.33%; 98.96%; and 100%) for the categories of BH (beach), BA (built-up area), VE (vegetation), WA (water bodies), and VE (vegetation, respectively) for the map of 2001. For the map of 2010, it ranged from 100% to 100% (100%; 100%; 100%; 100%, and 100% for BH, BA, VE, and WA, respectively). The user's accuracy of each class ranged from 91.67% to 100% in 2001 (91.67%; 86.21%; 96.96%; and 100% for BH, BA, VE, and WA, respectively). In 2021, it ranged from 100% to 100% (100%; 100%; 99.03%; and 100% for BH, BA, VE, and WA, respectively). The user's accuracy of Built-up area (BA) was the lowest among those of the four classes in 2001, with a value of 99.03%. In 2010, Vegetation was the lowest among those of the four classes, with a value of 99.03%.

4.1. Error Matrices for the 2001 Supervised Classification

Error Matrix				
	Reference Data			
Classified Data	**Beach**	**Build-up area**	**Vegetation**	**Water bodies**
Beach	55	5	0	0
Build-up area	2	25	2	0
Vegetation	2	0	191	0
Water bodies	0	0	3	34
Column Total	59	30	196	34

Accuracy Totals					
Class Name	Reference Totals	Classified Totals	Number Correct	Producers Accuracy	Users Accuracy
Beach	59	60	55	93.22%	91.67%
Build-up area	30	29	25	83.33%	86.21%
Vegetation	196	193	191	98.96%	98.96%
Water bodies	34	34	34	100%	100%
Totals	282	282	271		

Overall Classification Accuracy = 96.10%	
KAPPA (K^) STATISTICS	
Overall Kappa Statistics = 0.9181	
Conditional Kappa for each Category.	
Class Name	Kappa
Beach	0.8946
Build-up area	0.8456
Vegetation	0.9676
Water bodies	0.998

Table 3: Show Accuracy Assessment of Maximum Likelihood Supervised Classification for the Year 2001

4.1.1. Land Cover/Land Use Map

The land cover/land use distribution of 2001(fig 4.1) above showed that water accounted for the largest land cover/use of about 100% while vegetation had the second largest land cover/ use with 98.96%, Beach had 91.67%, and build-up area had 86.21%.

Error Matrix					
Reference Data					
Classified Data	**Beach**	**Build-up Area**	**Vegetation**	**Waterbodies**	
Beach	162	0	0	0	
Build-up area	0	52	0	0	
Vegetation	0	0	102	0	
Water bodies	0	0	0	45	
Column Total	162	52	102	45	
Accuracy Totals					
Class Name	Reference Totals	Classified Totals	Number Correct	Producers Accuracy	Users Accuracy
Beach	162	162	162	100.00%	100.00%
Build-up area	52	52	52	100.00%	100.00%
Vegetation	102	103	102	100.00%	99.03%
Water bodies	45	45	45	100.00%	100.00%
Totals	361	362	361		
Overall Classification Accuracy = 99.68%					
Conditional Kappa for each Category					
Class Name	Kappa				
Beach	1				
Build-up area	1				
Vegetation	0.9857				
Water bodies	1				

Table 4: Accuracy Assessment of Maximum Likelihood Supervised Classification for the year 2010

The land cover/land use distribution of 2021 (figure 4.1) below showed that the beach, built-up, and water bodies had a land cover/use of 100% each, and vegetation had 95.28%.

4.1.2. Summary of Land Cover /Land Use Area for 2001, 2010, and 2021

The classification results shown in table 4 above indicate the land cover/land use classes in 2001 as:

- Water bodies (100%),
- Vegetation (98.96%),
- Beach (91.67%),
- Build-up area (86.21%), respectively

In contrast, from 2001 to 2010, land use for water bodies remained 100%, and for vegetation, land use decreased from 100% to 98.96%, with beach decreasing from 100% to 91.67% and build-up area decreasing from 100% to 86.21%.

Then from 2010 to 2021, land use for water bodies remained 100%, while for vegetation, land use decreased from 99.03% to 95.33%, for beach, it remained 100%, and for built-up area, it remained 100%. These states reflect the multi-temporal change in Idah from 2001 to 2021.

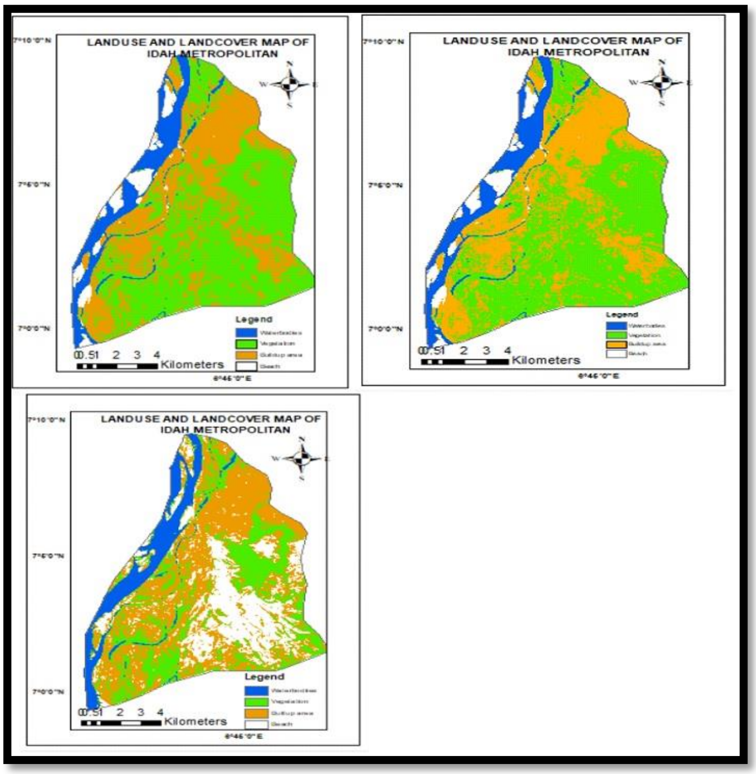

Figure 7: Land Use Map in (a) 2001(b) 2010 (c) and 2021

4.2. Change Detection Analysis

In order to evaluate the changes that have taken place from one land use land cover to another, a pair-wise comparison of the LULC output maps and their statistical inventories were made. The evaluation of the gains and losses, transitions between specific LULC categories, and contributions to net change experienced by each LULC type was generated using the Land Change modeler of Idrisi software, an initial state (2001) and final state (2021) images were not specified, and the land cover classes were matched to generate the statistics of change between them, following by from 2001 to 2010,and from 2010 to 2021. These land cover changes were computed between2001 and 2021.

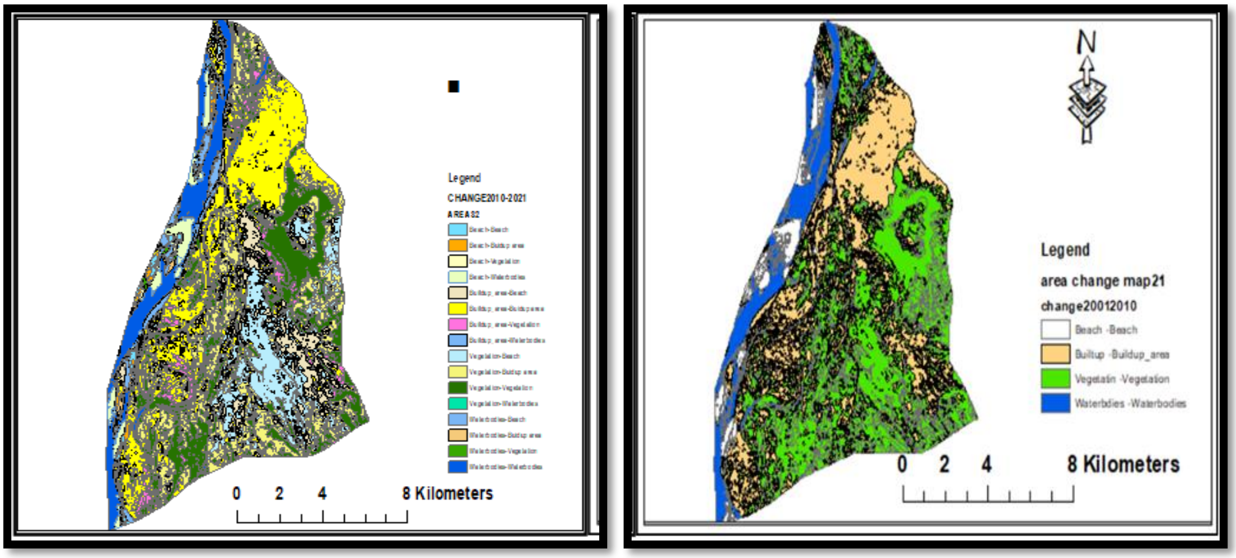

Figure 8: (a) Land Cover/ Land Change Detection between 2001 and 2010; (b) and 2010 and 2021

2001 to 2010		
Class Name	**Area(km sqr)**	**Percentage**
Decreased	30.23	22.51
Increased	93.08	69.33
Unchanged	10.95	8.16

Table 5: Per-Pixel Change between 2001 and 2010

2010 to 2021		
Class Name	**Area (km sqr)**	**Percentage**
Decreased	86.51	64.44
Increased	28.69	21.37
Unchanged	19.05	14.19

Table 6: Per-Pixel Change between 2010 and 2021

Tables 5 and 6 show the change detection statistics between 2001 and 2020. There was a drastic increase in the study area from 2001 to 2021 and the steady increase was observed up to 2010 (figure 8a). However, there was a sharp decrease observed from 2010 to 2021 (figure 8b).

4.3. Change Detection Based on the Supervised Classification

Further analysis was carried out on the supervised classification Classes found in the Idah. This was a need to ascertain these changes per class value. The table below shows the classification results from 2001 to 2021.

From 2001 To 2010		
Class	**% Change**	**Remark**
BEACH	28.1	INCREASE
BUILD-UP AREA	12.04	INCREASE
VEGETATION	49.98	DECREASE
WATERBODIES	9.87	INCREASE

Table 7: Change Detection between 2001 and 2010

From 2010 To 2021		
Class	**% Change**	**Remark**
BEACH	44.5	INCREASE
BUILD-UP AREA	1.33	DECREASE
VEGETATION	48.67	DECREASE
WATERBODIES	5.51	INCREASE

Table 8: Change Detection between 2010 and 2021

There were changes experienced in the various classes. The vegetated area experienced a great change of 49.98%. That is a decrease from the previous year of 2001 to 2010. Also, another 48.67% decrease from 2010 to 2021 is due to the developments in the study area. The Urban area equally decreased by 1.33 % between 2001 and 2010. There was an increase of 12.04% from the year 2010 to 2021. Beach has a drastic increase from 28.10% observed between 2001 and 2010 to 44.50% observed between 2010 and 2021.

5. Conclusion and Recommendations

This study aimed to examine urban change in the Idah metropolis of Kogi State during the years 2001, 2010, and 2021. The study first sought to identify changes in urban land cover before addressing possible mechanisms of urban land cover change. The study area's urban land cover was delineated using Landsat imagery. Then using a supervised Gaussian maximum likelihood classification, Landsat images were utilized to delineate the urban growth and modelling. An attempt was made to capture as accurately as possible four land use/ land cover classes as they change through time. The four classes we distinctly produced in contrast to urban development were for 2001, 2010, and 2021. An attempt was also made to generate the trend analysis to determine the trend of change percentage.

The result shows a significant change in build-up area between 2001 and 2010, showing a stage of modern urbanization and industrialization with water bodies slightly increasing from 2001 to 2021 and decreasing between 2021 and 2010 along with vegetation classes. In conclusion, these classes decrease as build-up area increases over the years, giving way for urbanization to grow.

6. References

i. Abubakar K. (2015) Land Use - Land Cover Changes and their implications in Nigeria using geo-spatial Techniques Unpublished. *Thesis in Remote Sensing and GIS in the Department of Geography, Ahmadu Bello University Zaria.April (2015).*

ii. Addis G. Y. (2009) Spatiotemporal Land Use/Land Cover Changes Analysis and monitoring in the balancing municipality, Spain M.Sc. *Thesis of WeslfalischeWithelms-University Munster, Germany Geo-spatial Technologies. March 2009.*

iii. Alves, H.P and Hogan, D.J. (2009). Demographic and Socio-economic Drivers of Deforestation in the Brazilian Atlantic Forest: A GIS Integration of Census and Remote Sensing Data at Different Spatial Scales. Paper Presented at the 7th International Science Conference on the Human Dimensions of Global Environmental Change, "*Social Challenges of Global Change"(IHDP Open Meeting 2009) held from 26–30 April 2009 in Born, Germany.*

iv. Augustine O.W. (2015) Geo-spatial Modelling and Multi-temporal analysis of urban development trends in Warri town Delta State Nigeria.*M.Sc Thesis of the Department of Surveying and Geoinformatics of NnamdiAzikiwe University Awka, Anambra State.*

v. Boori, M.S., Netzband, M., Choudhary, K. et al. Monitoring and modelling urban sprawl through remote sensing and GIS in Kuala Lumpur, Malaysia. Ecol Process 4, 15 (2015). https://doi.org/10.1186/s13717-015-0040-2

vi. Deep S., Sakland (2014) Urban SpewelModelling using Cellular Automate.*Egypt J. Remote Sensing and Space Science pp: 179–187.*

vii. Elizabeth A. Wentz, Sharolyn Anderson, MichailFragkias, MaikNetzband, Victor Mesev, Soe W. Myint, Dale Quattrochi, AtiqurRahman and Karen C. Seto, (2014) Supporting Global Environmental Change Research: A Review of Trends and Knowledge Gaps in Urban Remote Sensing: Remote Sens. 2014, 6, 3879–3905; doi:10.3390/rs6053879

viii. Enoquanbhor E.C, Florian G, Jonas O.N. Tobia L. and Blake B. W (2019) Land Cover Changes in the Abuja City, Region, Nigeria. Integrating GIS and Remoting Sensed Data to support land use planning.*Sustainability 11(5) 15:13*

ix. Enaruube G.O and Atedher G.O. (2015) Spatial Analysis of Agricultural land-use change in Asaba. *Ife Journal of Science Vol. 17 No.1*

x. Fosudo P.O and Ibrahim O.R. (2017) A Spatio-temporal Assessment of peri-urban agricultural land-use changes using a GIS overlay methodology of Kigali City, Rwanda. *https://www.researchgate.net 321.*

xi. Gobo A.E., Gordon A. and Agobie O.I (2018) Impacts of Urban land-use changes on Flood events in Warri Delta State Nigeria. *International Journal of Engineering Research and Application Vol.4 pg 48–60.*

xii. Merlyn S., Nabo H., Ronald G., Aldrin J.H, Aldrin A. and Cristino (2019) Land

xiii. Use/Land Cover Change Detection and Urban Spraw/Analysis in the mount making Buffer Zone, Philippines.*Environments 2019 6, 9.*

xiv. Odjugo P.A, Enardube O. and G.O. Isibor H. (2015) The Spatio-temporal pattern of urban growth in Benin City Nigeria. *African Journal of Environmental Science.Vol 9(3) pp 166–175.*

xv. Ogunjobi K.O., Adamu Y. Akinsanola A.A and Orimoloye I.R (2018) *Spatiotemporal analysis of land use dynamics and its potential indications on land surface temperature in Sokoto Metropolis, Nigeria Royal Society Open Sciences.*

xvi. Peter C.C., Chibuike C. Alozie M.C, Agbaze U.O and Obasi C.E. (2017) Spotio – Temporal Analysis of Land Use Dynamics using Change Detention Analysis.*International Journal of Advanced Research in Science, Engineering and Technology Vol.4*

xvii. Subasinghe, S.; Estoque, R.C.; Murayama, Y. Spatiotemporal Analysis of Urban Growth Using GIS and Remote Sensing: A Case Study of the Colombo Metropolitan Area, Sri Lanka. ISPRS Int. J. Geo-Inf. 2016, 5, 197. https://doi.org/10.3390/ijgi5110197

xviii. Shanmugam T. And Rajagopalan B. (2011). Detecting Urban Change of Salem City of Tamil Nadu, India from 1990 to 2010 Using Geo-spatial technology. *International Transaction Journal of Engineering, Management, & Applied Sciences & Technologies vol 2 no. 2 in 2228–9860.*

xix. Yadav P.K, Mohnish K, Kiranmay S.I (2012) Land Use, Land Cover Mapping, Change Detection and Conflict Analysis of Nagzira – Mavegaon Corridor, Central India using geo-spatial Technology. *International Journal*